11466 Advanced Polymeric Coatings and Their Applications: Green Tribology

Pixiang Lan, ATSP Innovations, Champaign, IL, United States

Emerson E Nunez, Universidad Autónoma de Occidente, Cali-Valle, Colombia

Andreas A Polycarpou, Texas A&M University, College Station, TX, United States

Introduction

Recent advances in polymer engineering, such as new emergency materials and new coating technologies enable broader applications of polymeric coatings. Three types of functional coatings, namely tribological coatings, hydrophobic coatings and self-healing coatings have been widely investigated, and summarized in this article.

Tribology has emerged as a field that contributes to the development and implementation of materials that are sustainable, from an energy and environmental point of view. Sustainable materials from the point of view of green tribology are those materials that can diminish friction and wear of interacting surfaces, minimize heat dissipation, and thus lower pollution. Through the development of self-lubricating materials, wear can be minimized and contribute to a greener environment by increasing the life cycle of sliding materials (tribopairs), causing a positive impact in environmental degradation, by decreasing the waste and recyclability cycle (Sasaki, 2010; Anand *et al*., 2017). Environmentally friendly tribomaterials in the form of self-lubricating advanced polymeric coatings contribute to a greener environment by reduction or complete elimination of liquid lubricants at the sliding interfaces, thus reducing emissions, and in turn less pollution to the atmosphere.

High bearing polymer coatings based on PEEK, PTFE, ATSP and their blends have emerged as a cost-effective solution for friction and wear problems of sliding interfaces that must operate in the absence of lubricant. Experimental results show that the friction coefficient (COF) at a polymer/metal interface is governed by solid lubrication in the form of third bodies, even at values lower than those found in metal/ metal interfaces in the boundary and mixed lubrication regimes (Demas and Polycarpou, 2008; Nunez *et al*., 2010; Akram *et al*., 2013), thus contributing to a greener environment (less power consumption). In addition, these advanced polymeric coatings have been applied in aggressive tribological applications, such as cryogenic conditions, and in space applications, where materials have to be able to withstand sliding under non-traditional conditions, making their design challenging (**Gao *et al*., 2018**). The purpose of this book chapter is to provide an insight of the recent trends in the design of advanced high bearing blended polymer coatings, as viable candidate solutions for aggressive tribological applications in demanding contemporary industries, and their contribution to a greener environment.

Superhydrophobic coatings exhibit low surface energy, and when water rests or slides on the surface, it absorbs dust and together slide off the surface: this phenomenon is called self-cleaning. The self-cleaning property can save cost for cleaning, when superhydrophobic coatings are applied on surfaces such as solar panels and windows. In addition, superhydrophobic coatings can enhance anticorrosion properties by separating water in contact with metal substrates. When coatings are in service, they are prone to damage due to their thin section: once damage occurs, the coatings will lose their functionality such as anticorrosion. Thus, by applying self-healing coatings that can repair themselves is attractive; by self-healing, the coatings will have a longer service life and there is no need to re-apply them when they experience damage.

Polymer Coating Deposition Techniques for Advanced Tribological Applications

Polymer coating deposition on a wide variety of engineering substrates has gained significant attention. Coatings are tailored to provide specific characteristics, such as wear, corrosion, chemical and weathering resistance, to improve thermal conductivity, to provide electrical insulation, and in the case of some polymers, to provide solid lubrication and low friction. Thermal spray (TS) and cold dynamic spray or simply cold spray (CS) are the main techniques employed to coat polymers onto substrates.

Among the main advantages of TS are: (a) the feasibility to coat large components of complex geometries, (b) the use of powder as raw material (eliminating the use of solvents), and (c) the possibility of the technique being applied in the field, to coat and/or repair a component. Depending on the physical principle employed for deposition, TS techniques can be subcategorized as shown in **Fig. 1**. For instance, in TS,

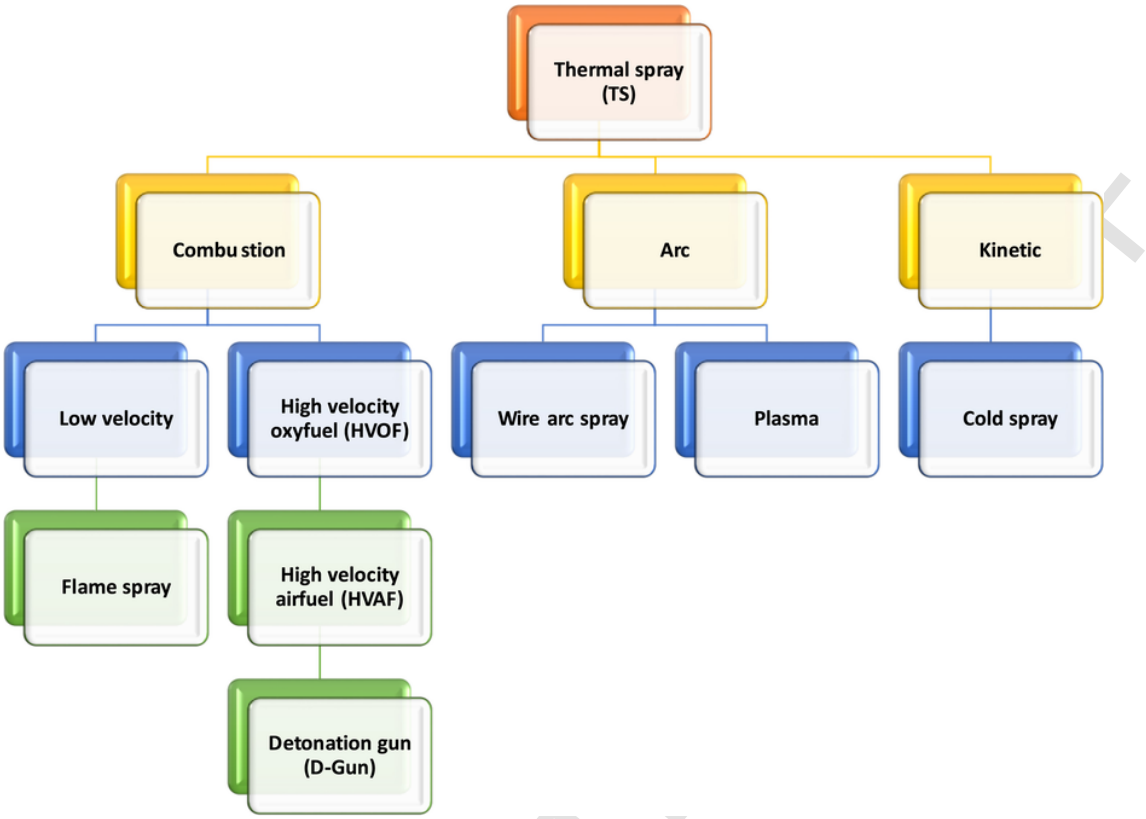

Fig. 1 Thermal spray deposition techniques and subcategories. Modified from Wen, C., 2015. Surface Coating and Modification of Metallic Biomaterials. Woodhead Publishing.

deposited polymer material in powder form adheres to the substrate by a high velocity and high temperature thermal jet produced by electrical or chemical energy. This energy is used to heat, melt, and spray the molten material introduced in the flame through a nozzle, before impacting the target surface. Once the particles impact the substrate, they solidify and form the coating by superposition (**Petrovicova and Schadler, 2002**).

In CS the amount of energy (electric or calorific) required to accelerate the particles to the substrate is lower, compared to TS. In fact, the name CS refers to the range of temperatures employed during the flow of the gas through the nozzle, which can vary from −100 to 100°C (**Raletz *et al*., 2006**). In CS, due to the relatively low temperature process, which is usually lower compared to the melting point of the powder, the adhesion forces between the deposited powder and substrate, along with the cohesion forces between the powder particles in the solid state, make this process remarkable. In fact, due to the low temperature and the absence of oxidation, the final coatings produced by CS not only have lower residual stresses and porosity, but higher bond strength, compared to TS techniques (**Champagne and Helfritch, 2014**). Unlike TS, CS can be performed at standard pressure, temperature, and humidity, simplifying the operating conditions.

According to **Fig. 1**, TS deposition methods for polymer coatings are classified depending on the energy source employed to accelerate the powder particles towards the substrate. As shown in **Fig. 1**, powder flame spray, arc wire, plasma, high velocity oxyfuel (HVOF), and CS are considered the most popular TS polymer coating deposition techniques, where the final coating thickness ranges from tenths of micrometers to several millimeters (**Bach *et al*., 2006**).

Fig. 2(a) shows a schematic of the wire flame spray, where a concentrical wire material is driven and reacts with an oxygen-fuel rich gas flame. As a result, the material is melted and sprayed towards the substrate to be coated. Similarly, in powder flame spray, the wire is replaced by a polymer powder which reacts with the flame and reaches the substrate to form the coating. Plasma is another TS process that can be used for the deposition of polymer coatings. As shown in **Fig. 2(b)**, an arc of high frequency develops between a cathode (usually tungsten) and anode, ionizing the gas flowing through the electrodes (for instance He, N_2, H_2). As a result of this process, the temperature of the plasma can reach up to approximately 25,000°C and is used to melt the powder material and accelerate it towards the substrate (**Davis, 2001**).

Surface preparation is one of the key aspects to avoid delamination of the coating to the substrate. This process is usually performed by roughening the substrate by using grit blasting, which increases the surface roughness. As a result, the exposed surface of the substrate is activated by an increase in free surface energy which improves the bonding between the impacting polymer particles and the substrate (Fender, 1996; Vyawahare, 2006). In CS, powder polymer particles reach and bond to the substrate in solid state by the acceleration of the gas that passes through a convergent-divergent nozzle (**Assadi *et al*., 2011**).

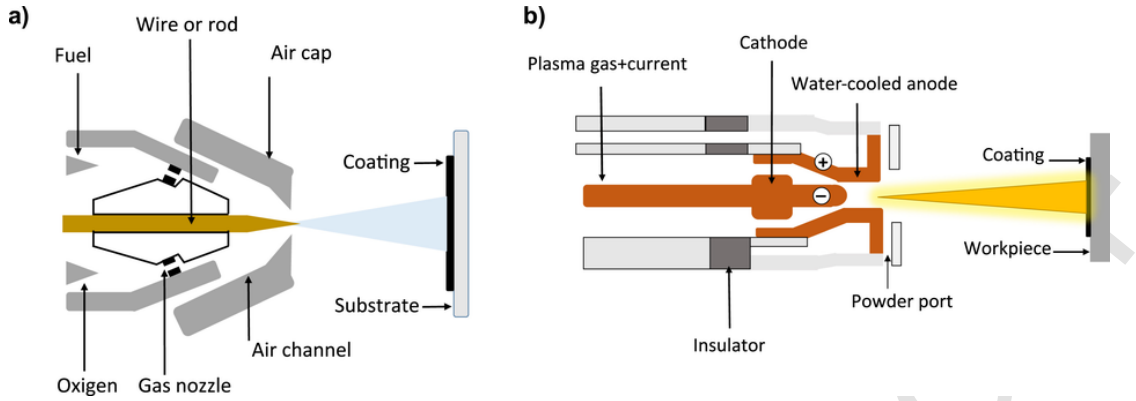

Fig. 2 Thermal spray deposition techniques: (a) Wire flame spray, (b) plasma spray. Modified from Davis, J.R., 2001. Introduction to thermal spray processing. In: Handbook of Thermal Spray Technology, 3–13. ASM Innternational and Thermal Spray Society.

Different types of polymers for advanced tribological applications can be applied using the aforementioned techniques. These polymers are classified on a pyramid, based on their mechanical properties, operating temperatures and cost (see **Fig. 3**) (**Friedrich, 2018**). On top of the pyramid shown in **Fig. 3**, polymers such as Polyetheretherketone (PEEK), Polyimides (PI), Polyamide-imide (PAI), Polytetrafluoroethylene (PTFE) and aromatic thermosetting copolyester (ATSP) (Frich *et al*., 1996; Frich and Economy, 1997; Zhang, 2008; Lan *et al*., 2016) are designed for tribological problems, and are commercialized as powders, where their size ranges from 10 to 180 µm (**Berretta *et al*., 2014**).

As shown in **Fig. 4**, polymer powder can be obtained using cryogenic mechanical grinding. Tribological studies of high performance thermoplastic polymer coatings, show that flame spray, HVOF, plasma, electrostatic deposition and CS are the most popular techniques to deposit a variety of high-performance polymers (HPPs). For instance, through annealing treatment and holding time of the substrate, it was shown that PEEK coatings deposited on Al substrates by flame spraying showed higher crystallinity. Thus, higher hardness and wear resistance, compared to those treated with lower annealing temperature (**Zhang *et al*., 2006b**). Other studies, also show the benefits of substrate pretreatment by *Nd:YAG* (*neodymium-doped yttrium aluminum garnet*) and CO_2 infrared lasers; these treatments provide advantages compared to conventional grit blasting, especially for brittle materials. Laser surface pretreatment has the advantage of delivering a significant amount of power on a small area of the work piece, without compromising the bulk properties of the substrate. These pretreatments, also reduce the heating time (compared to flame and induction heating) of the substrate, and improve the mechanical properties of the final coatings (**Zhang *et al*., 2006a**). It was proven that treatment with CO_2 laser improved densification of the PEEK coating, leading to less porosity and higher mechanical properties, compared to Nd:YAG laser treatment.

Polymer coating deposition is also carried out using electrostatic spraying, where the polymer powder is electrostatically charged under low current (in the µA range) and voltage (30–90 kV) and applied onto the electrically grounded substrate. There is abundant literature related to tribological studies of HPPs deposited using electrostatic deposition. These studies were mainly focused on deposition of blended PEEK, PI, PTFE, and ATSP polymer powders deposited onto substrates such as gray cast iron, Al390-T6, sintered iron, and Mn-Si brass, which are

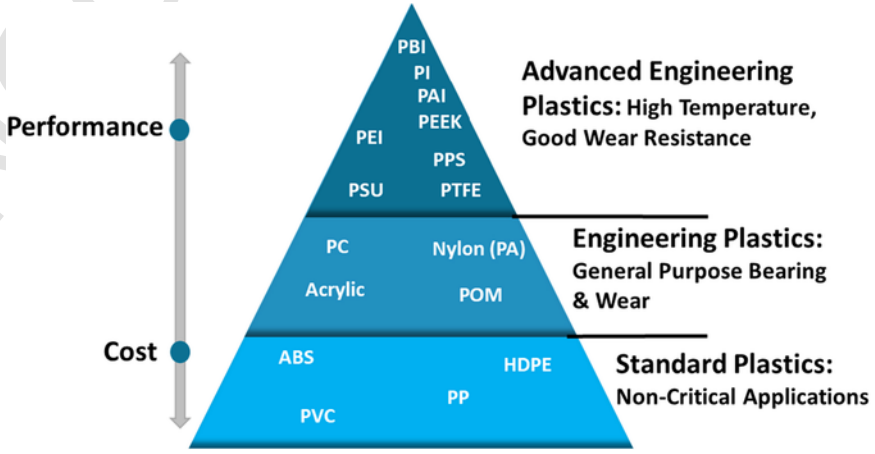

Fig. 3 Polymer pyramid listing high performance polymers used in TS processes organized from amorphous to crystalline. Modified from Friedrich, K., 2018. Polymer composites for tribological applications. Advanced Industrial and Engineering Polymer Research 1, 3–39.

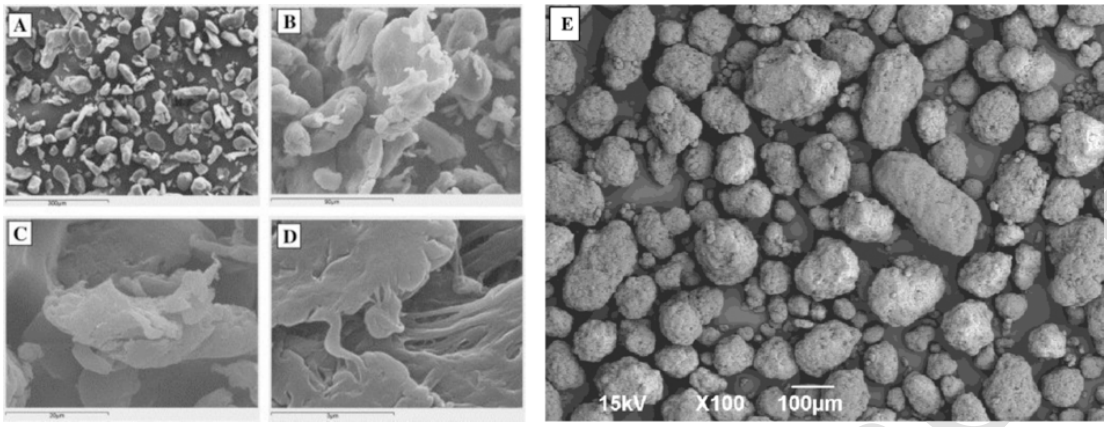

Fig. 4 SEM microscopy images of PEEK powder (A–D), and (E) polymer powder of Ultra high molecular weight polyethylene (UHMWPE). Modified from Berretta, S., Ghita, O., Evans, K.E., 2014. Morphology of polymeric powders in Laser Sintering (LS): From polyamide to new PEEK powders. European Polymer Journal 59, 218–229.

found in different air-conditioning and refrigeration components, as well as electrical submersible pumps (ESPs) (Shaffer and Rogers, 2007; Demas and Polycarpou, 2008; Dascalescu *et al*., 2009; Nunez *et al*., 2010; Nunez *et al*., 2011; Yeo and Polycarpou, 2012; Lan *et al*., 2017; Lan *et al*., 2018; Lan and Polycarpou, 2018; **Nunez *et al*. 2019**). Deposition of the aforementioned HPPs as coatings through electrostatic deposition, and tailored for tribological applications has proven to be effective and inexpensive, compared to other techniques. However, deposition techniques, such as CS spray eliminate the curing process, required in the electrostatic technique.

Fig. 5 shows typical cross-sectional images of different polymer coatings obtained by electrostatic deposition. It can be seen that the typical thickness of the coatings is of the order of tenths of microns (**Nunez *et al*., 2011**). The list of polymers that can be sprayed onto

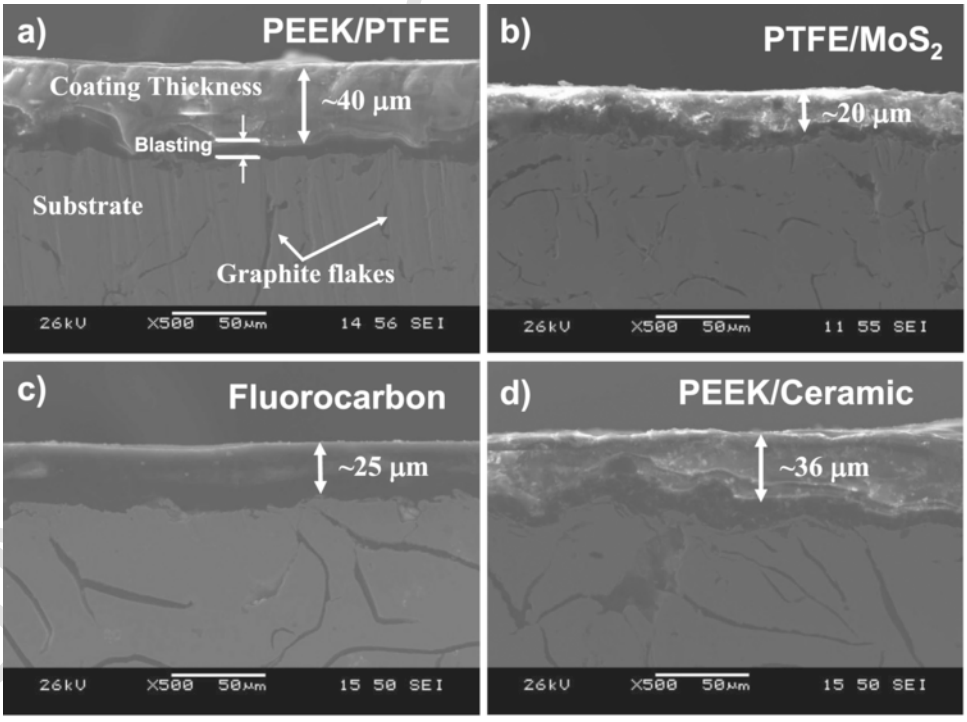

Fig. 5 Cross sectional SEM images of typical HPP coatings: (a) PEEK/PTFE, (b) PTFE/MoS_2, (c) Fluorocarbon, (d) PEEK/Ceramic deposited on gray cast iron by electrostatic deposition. Modified from Nunez, E.E., Yeo, S.M., Polychronopoulou, K., Polycarpou, A.A., 2011. Tribological study of high bearing blended polymer-based coatings for air-conditioning and refrigeration compressors, Surface and Coatings Technology 205 (8–9), 2994–3005.

different substrates using different TS techniques is listed in reference (**Petrovicova and Schadler, 2002**). There are other techniques such as spin coating and dip coating that can be used for the deposition of uniform thin polymer films (from few nanometers to few micrometers) on different substrate materials, and are used in different sectors, such as the semiconductor and biomedical industries. However, coatings developed using these techniques are not specifically designed to address tribological issues (**Danglad-Flores *et al*., 2018**).

Tribology of Polymer Coatings under Extreme Working Conditions

Increasing demand of advanced materials that can withstand extreme operating conditions in several industries, has called the attention of the polymer industry for the development of composites and blends that can perform well under difficult or extreme working conditions. For instance, spacecrafts and satellites are exposed to cosmic rays, impact of debris from spacecraft and meteoroids, ultra violet radiation, vacuum, microgravity, thermal cycling, and cryogenic conditions, which make the design and selection of materials for these applications challenging (Pippin, 2003; Kondyurina *et al*., 2006; Wang *et al*., 2016; Gao *et al*., 2018). In the air-conditioning and refrigeration industry there has been interest in oil-less compressors, mainly due to the negative thermodynamic effect from the liquid lubricant/refrigerant mixture in the refrigeration cycle. The mixture not only decreases the thermodynamic efficiency, but under boundary/mixed lubrication conditions, it can affect the properties of the lubricant causing scuffing on the sliding components (Demas *et al*., 2005; Cannaday and Polycarpou, 2006; Nunez *et al*., 2008; Akram *et al*., 2014).

Another industry where harsh operating conditions cause tribological issues, is the oil and gas industry. In this regard in ESPs, high bearing loads and high temperature can cause failure of the lubricant film in the hydrodynamic bearings, causing a transition from hydrodynamic to boundary and mixed lubrication regimes. As a consequence, interactions of the asperities of the pad bearings might cause seizure, leading to scuffing at the bearing contact interface (Wang, 1997; Lan *et al*., 2017). As stated above, advanced thermoplastic polymers can be used to coat different substrates in the tenths of micrometer thickness. One of the main advantages of high bearing blended polymer coatings, is not only the fact that they can provide solid lubrication in the form of third bodies under unlubricated conditions (in the absence of liquid lubricant), but also the fact that they provide a low cost/efficiency ratio (Yeo and Polycarpou, 2012, 2013).

We have been broadly studying the tribological performance of high bearing load blended polymer coatings based on PEEK, PTFE, and ATSP for different industrial applications; Testing instruments include specialized custom-made tribometers, which are capable to carry out tests at high normal loads (up to 5000 N), high temperatures (from 120 up to 1000°C) and high pressures up to 13.8 MPa (**Dascalescu *et al*., 2009**). In the air-conditioning and refrigeration industry the studies have been focused on the replacement of sliding components. Namely, Al390-T6, Mn-Si brass, which are used in automotive swash plate compressors, and gray cast iron, and sintered iron, commonly found in scroll and piston compressors, respectively (**Yeo *et al*., 2010**).

Three different commercially available PTFE-based coatings deposited onto gray cast iron disks (Dura-Bar G2); namely, DuPont® 958–303, DuPont® 958–414 and Whitford Xylan® 1052, all of them with thickness of approximately 20–30 μm (see **Fig. 6**), were tested against 52100 steel, under unlubricated conditions (**Demas and Polycarpou, 2008**). The first two coatings were PTFE/pyrrolidone based, while the latter was PTFE/MoS_2. These coatings were tested under reciprocating motion (±30° at a frequency of 4.5 Hz) to simulate the

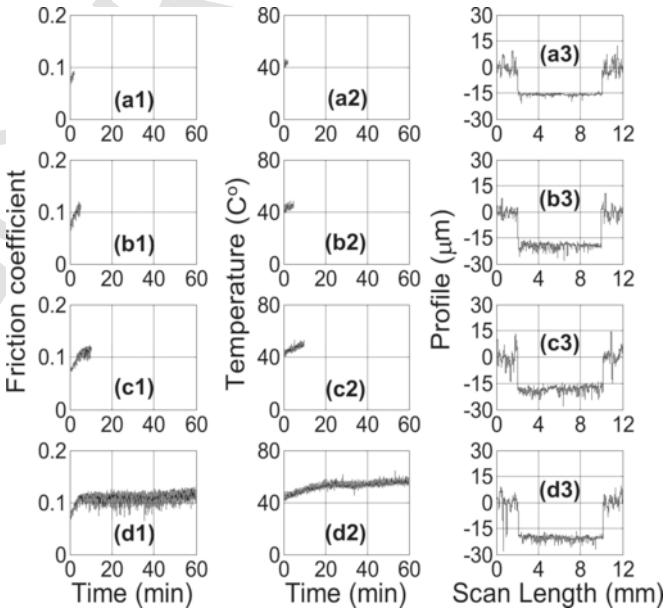

Fig. 6 Friction coefficient, near contact temperature and profilometric measurements for experiments performed at 2 (a1–a3), 5 (b1–b3), 10 (c1–c3) and 60 (d1–d3) mins for DuPont® 958–303 in CO_2 atmosphere at 445 N. Modified from Demas, N.G., Polycarpou, A.A., 2008. Tribological performance of PTFE-based coatings for air-conditioning compressors. Surface and Coatings Technology 203 (3–4), 307–316.

contact of the wrist pin and the piston in a piston-type compressor. Under aggressive loading conditions (460 MPa Hertzian line contact pressure), the experimental results show that scuffing at the interface was retarded due to the action of third bodies coming from the wear debris. This debris was kept trapped at the contact interface and retarded scuffing by the action of solid lubrication. This was proved after running experiments at 2, 5, 10, and 60 min, where it was shown that most of the wear took place during the running-in transient period, by comparing wear depth contact profilometry measurements against the thickness of the coatings, being in all cases around 20–30 μm (see **Fig. 6**). These results proved that advanced polymer coatings could potentially be applied in situations of high contact stresses under unlubricated conditions, being a relatively cheaper solution compared to hard diamond-like carbon (DLC) coatings (Grill, 1993; Donnet and Erdemir, 2004).

Studies were performed to understand the feasibility of applying the aforementioned coatings on Al390-T6, gray cast iron, and sintered iron substrates (**Yeo *et al*., 2010**). It was proved through X-ray Photoelectron Spectroscopy (XPS), that Al390-T6 was difficult to coat and that PTFE/MoS_2 was the only polymer material capable to adhere onto this substrate, and also the only one which did not suffer severe scuffing (**Dascalescu *et al*., 2009**). It can be seen in the XPS spectra of **Fig. 7(a)**, that fragmentation of PTFE enabled its interaction with the Al390-T6 substrate. As a result, this chemical interaction improved the adhesion of PTFE to the substrate, based on the C-species peaks at 292 eV, related to PTFE (which is found as a peak in the F1s core level spectra analysis (**Fig. 7(b)**)). It was proven that under unlubricated sliding conditions, these coatings provide solid lubrication through their ability to form transfer films, making them an attractive solution to replace metal tribopairs in oil-less engineering applications (Ovaert and Cheng, 1991; Bahadur, 2000; Nunez and Polycarpou, 2015).

Feasibility of deposition of these commercial coatings onto different engineering substrates is summarized in **Table 1**. Micromechanical properties of these coatings were also obtained using a TI-950 TriboIndenter (**Yeo and Polycarpou, 2013**). The elastic modulus and hardness as a function of contact depth is shown in **Fig. 8**. It can be seen that all coatings show consistent values of reduced elastic modulus (E_r) and hardness (H) at shallow contact depths (1.5–2.0 μm), except for the case of the PEEK/PTFE coating, with its behavior is attributed to significant pile-up. **Fig. 9** shows the wear rates of the same coatings under both oscillatory and unidirectional sliding conditions. It can be observed that there are higher wear rates and COF values under oscillatory conditions, compared to unidirectional sliding, for the same polymer coating. This can be explained by the fact that temperature at the sliding interface is governed by the sliding speed and normal load, which is higher under unidirectional sliding, compared to small amplitude oscillatory sliding. It is expected that under high temperature, adhesion and material transfer will be enhanced due to higher adhesion which ends up in lower wear rates. Also, under oscillatory conditions, material has to be replenished due to the back and forth sliding motion, decreasing material transfer efficiency (**Yeo and Polycarpou, 2014**).

Studies on the performance of polymer coatings designed for tilting pad bearings in ESPs have also been performed. C182000 chrome-copper disks were coated by electrostatic deposition with ATSP/PTFE (Zonyl® MP1100) blends (**Lan *et al*., 2017**). ATSP-based coatings were compared to PEEK-based coatings (1704 PEEK/PTFE) deposited on the same substrate by an authorized vendor (see **Table 1**), and both tested against AISI 4130 steel and C932000 bronze cylindrical pins. The experiments were carried out under hydrodynamic lubrication in an abrasive three body (silica) sand (2 wt% silica sand #140) and ISO 46 mineral oil to simulate the conditions of the contaminated lubricated system. The experiments were performed at a nominal contact pressure of 6 MPa with a duration of 30, 80, and 120 min at a sliding speed of 1.9 m/s. It was shown that friction coefficient was lower for PEEK/PTFE coating, compared to ATSP, due to the lower initial roughness of the

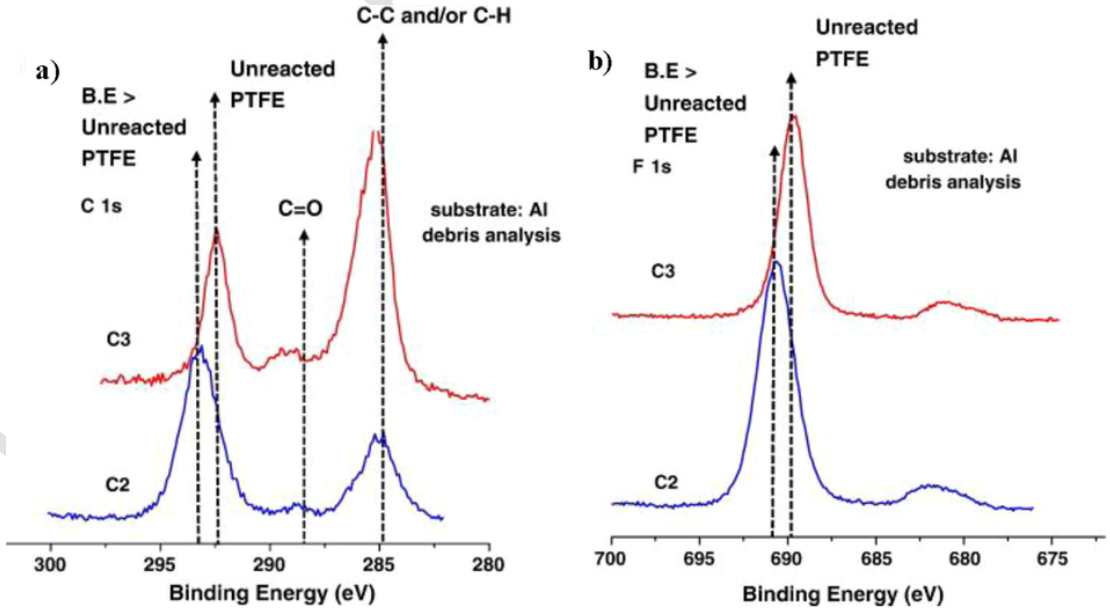

Fig. 7 Analysis of the wear debris after tribotesting of AISI 52100 steel pins against Al390-T6 coated with DuPont® 958-414 (coating C2) and Whitford Xylan® 1052 (coating C3) by XPS core level spectra (a) C1s; (b) F1s. Modified from Dascalescu, D., Polychronopoulou, K., Polycarpou, A., 2009. The significance of tribochemistry on the performance of PTFE-based coatings in CO_2 refrigerant environment. Surface and Coatings Technology 204 (3), 319–329.

Table 1 List of different commercial polymer coatings and engineering substrates

Coating material	*Vendor*	*Substrate material compatibily*				*Thickness (μm)*
		Al390-T6	*Gray cast iron*	*Sintered iron*	*Chrome copper C182000*	
PEEK/PTFE	Southwest Impreglon	Good	Excellent	Excellent	Excellent	30–40
PTFE/MoS_2 (Fluorolon® 325)	Southwest Impreglon	Good	Excellent	Excellent	–	20–30
Fluocarbon (Impreglon® 218)	Southwest Impreglon	Poor			–	20–30
PTFE/Pyrrolidone-1 (DuPont® 958–303)	DuPont®	Poor	Excellent	Excellent	–	20–30
PTFE/Pyrrolidone-2 (DuPont® 958–414)	DuPont®	Poor	Excellent	Excellent	–	20–25
PTFE/MoS_2 (Whitford Xylan® 10–52)	Whitford®	Excellent		Excellent	–	15–20
ATSP/PTFE	ATSP Innovations	–	Excellent	Excellent	Excellent	20–30

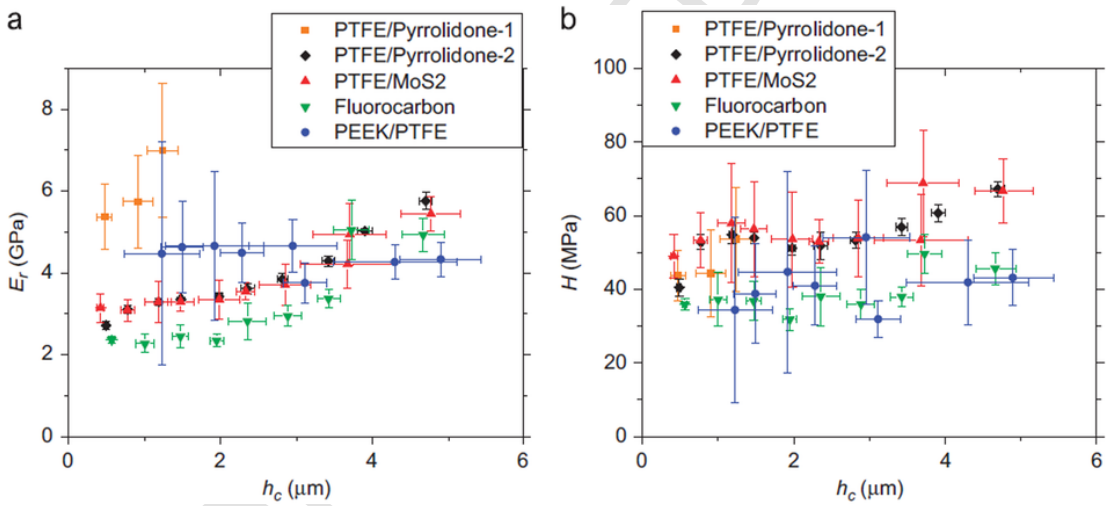

Fig. 8 (a) Reduced elastic modulus and (b) Hardness vs contact depth for five different commercial polymer coatings. Modified from Yeo, S.M., Polycarpou, A.A., 2013. Micromechanical properties of polymeric coatings. Tribology International 60, 198–208.

PEEK/PTFE. Wear rates were lower in case of ATSP tested with smaller sand size, compared to the case of larger #140 sand. This behavior was attributed to the interaction of smaller sand particles at the contact interface when compared to larger size particles (**Myshkin *et al.*, 2005**). Overall, considering the three different materials tested, ATSP exhibited the lowest wear rate followed by C18200 (chrome-copper), and PEEK/PTFE.

The tribological performance of polymer coatings under cryogenic conditions is of great importance for some industries. For instance, the advent of liquid hydrogen (LH_2) to power rockets and engines poses new challenges in the research of materials that can withstand harsh conditions at very low temperature (**Friedrich *et al.*, 2009**). The behavior of PTFE at cryogenic temperatures was studied at two different temperatures; namely room temperature (RT) and 77 K. It was shown that wear debris of PTFE at RT was governed by creep and shear stresses due to plowing; however, at −196°C abrasion is the main wear mechanisms and wear rate decreases due to an increase in surface hardness (**Michael *et al.*, 1991**). Tribological performance of ATSP and PEEK based coatings deposited on gray cast iron and tested at −40°C, −100°C and −160°C using a specialized tribometer at normal loads of 5 and 10 N was investigated. No measurable wear was obtained after testing of ATSP and PEEK, and the COF was higher in the PEEK material tested at different cryogenic experimental temperatures. Also, after

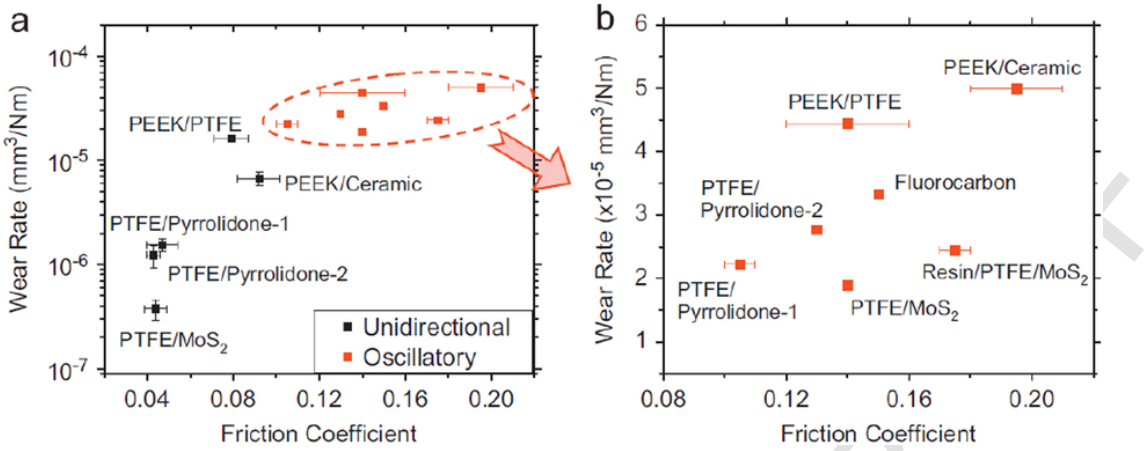

Fig. 9 Friction coefficient vs. wear rate of different PEEK and PTFE blended polymer coatings in CO_2 (22°C and 0.17 MPa) environment at 445 N normal load under both; unidirectional and dry-oscillatory conditions. Modified from Yeo, S.M., Andreas. A.P., 2012. Tribological performance of PTFE-and PEEK-based coatings under oil-less compressor conditions. Wear 296, 1–2, 638–647.

testing, cracks were observed on the wear tracks and they were related to the elastic modulus of the polymer coatings, where a more ductile PEEK was easier to plastically deform resulting in less microscopic cracks, compared to ATSP.

Hydrophobic Coatings and Their Applications

When a water droplet contacts with a rough solid surface, a contact angle (CA) forms, which is the angle that forms with the vertex located at the three-phase (liquid–vapor-solid) common point: one arm is the liquid-solid interface and the other arm is the liquid-vapor interface, as shown in **Fig. 10**. When the CA is smaller than 90°, as shown in **Fig. 10(a)**, the solid surface is a hydrophilic surface, which means the solid surface has high surface energy and is able to attract water and wet the surface. **Fig. 10(b)** shows a hydrophobic surface that has a CA larger than 90°; the hydrophobic surface has a low surface energy and repels water and resists wetting. When the CA is larger than 150°, the surface is called superhydrophobic surface. The CAs denoted in **Fig. 10(a) and (b)** are in static condition; once the droplet is in dynamic condition, the contact angle is in a range between receding contact angle (θr) and advancing contact angle (θa), as shown in **Fig. 10(c)** on a titling surface. The contact angle hysteresis (CAH) is equal to the advancing contact angle (θa) minus the receding contact angle (θr). When the adhesion between the solid and liquid is low, the CAH is small, and vice versa. Thus, the CAH is an important parameter characterizing adhesion, wetting, and energy dissipation during droplet flow (**Nosonovsky and Ramachandran, 2015**).

The lotus leaf is well-known for its superhydrophobic and self-cleaning property. **Fig. 11** shows three different magnifications of SEM images of a lotus leaf surface. **Fig. 11(a)** with the lowest magnification shows the surface microstructure, which is formed by papillose epidermal cells. After zoom in, a fluffy structure covering the micro-size cell is revealed, as in **Fig. 11(b)**. With further zoom in, the fluffy structure is revealed and shows nano epicuticular wax tubules, as in **Fig. 11(c)** (**Koch *et al.*, 2009**). Surfaces with non-polar or less polar material have low surface energy, and such materials include hydrocarbon components of epicuticular waxes. For the lotus leaf, with the nano epicuticular wax tubules as in **Fig. 11(c)**, air is enclosed in the nano structure and forms an air nano tubule composite surface. This composite surface results in low surface energy by increasing the water/air interface and decreasing the solid/water interface.

With large CA, the water is hard to wet the surface and the water droplet forms a near spherical geometry (**Barthlott and Neinhuis, 1997**). Dirt particles resting on the lotus leaf are usually larger than the surface microstructures, which means that the real solid-solid contact area is

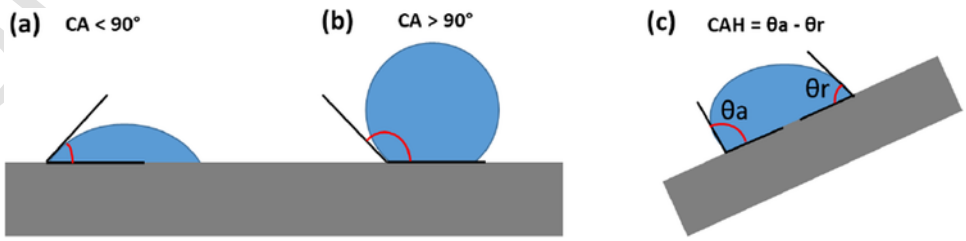

Fig. 10 Presentation of contact angles: (a) Hydrophilic surface, contact angle (CA)<90°, (b) hydrophobic surface, CA>90°, (c) on a tilting surface, contact angle hysteresis (CAH) = advancing contact angle (θa) − receding contact angle (θr).

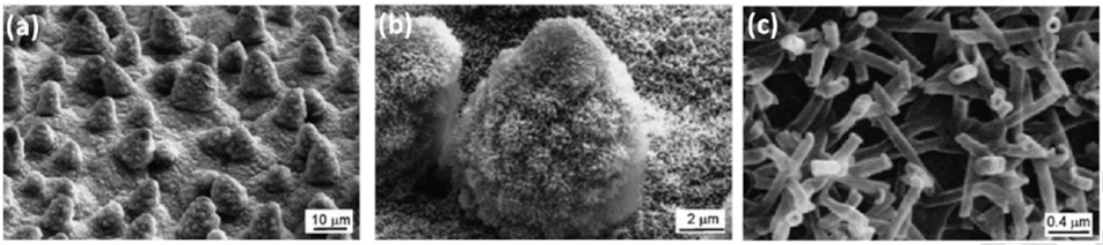

Fig. 11 SEM micrographs with three magnifications on Lotus leaf surface, which consists of a microstructure formed by papillose epidermal cells covered with epicuticular wax tubules on the surface, which create nanostructures. Modified from Koch, K., Bhushan, B., Jung, Y.C., Barthlott, W., 2009. Fabrication of artificial Lotus leaves and significance of hierarchical structure for superhydrophobicity and low adhesion. Soft Matter 5 (7), 1386–1393.

small and the adhesion force is also small. Thus, the particle material is more readily wetted by water compared to the epicuticular wax. When the particles encounter the rolling water droplet, the particles are ready to be absorbed by the water droplet and be detached and removed from the lotus leaf (**Barthlott and Neinhuis, 1997**). Inspired by the micro/nano structure of lotus leaf, artificial coatings have been developed to possess functions such as self-cleaning (Nine *et al*., 2015; Fenero *et al*., 2017; Selim *et al*., 2017; Xiao *et al*., 2017; Selim *et al*., 2018b), enhanced antifouling (Selim *et al*., 2017; Selim *et al*., 2018a; Selim *et al*., 2018b), fluid drag reduction (Dong *et al*., 2013; Srinivasan *et al*., 2015), and deicing (Arianpour *et al*., 2016; Nazhipkyzy *et al*., 2016; Nine *et al*., 2017). A common method to produce artificial hydrophobic coatings is to use polymers as a binding agent and add different micro/nano particle materials to form the micro/nano structured surfaces (Nine *et al*., 2015; Fenero *et al*., 2017; Selim *et al*., 2017; Xiao *et al*., 2017; Selim *et al*., 2018b).

For self-cleaning, the CA should be large, the CAH should be small, and the surface should be formed by a non-polar material. In addition, the hydrophobic coating should have good abrasion/scratch resistance to ensure good durability (**Nine *et al*., 2015**), and antistatic capability to dissipate static electricity (as static electricity is prone to absorb small dirt particles (**Fenero *et al*., 2017**)). To maintain superhydrophobicity, the key is to maintain the micro/nanostructure, and this could be accomplished using a high wear resistance material, or by wear of the surface layer, but exposing new nanostructure underneath. **Nine *et al*. (2005)** designed graphene-based superhydrophobic composite coatings with robust mechanical strength, and their tests showed that superhydrophobicity was retained even after sandpaper abrasion and crosscut scratching. In another study, by using a high scratch resistance oxide La_2O_3, **Xiao *et al*. (2017)** synthesized coatings that maintained their nanostructure and superhydrophobicity after 80 cycles of sand abrasive sliding. Another terminology worth mentioning is omniphobicity, which describes a surface that has repellent property for both polar and non-polar liquids (such as water, oil, methanol, octane, crude oil and blood), enabling the so called "full self-cleaning" characteristics (Tuteja *et al*., 2008; Wong *et al*., 2011; Fenero *et al*., 2017). These omniphobic surfaces could be used for biomedical fluid handling, fuel transport, self-cleaning windows and optical devices (**Wong *et al*., 2011**).

After immersion in seawater, ships will have biofouling on their hulls, thus will increase the fluid drag and fuel consumption (**Selim *et al*., 2018b**). Fouling release agents such as Ag nanoparticles, copper and/or booster biocides are commonly used in antifouling paints. When antifouling paints are produced into hydrophobic surfaces, the antifouling performance can be effectively enhanced by inhibiting fouling adhesion and the self-cleaning properties (Selim *et al*., 2017; Selim *et al*., 2018a; Selim *et al*., 2018b). In addition, as water can easily move on hydrophobic surfaces, it can decrease the shear force between the water and the surface (**Srinivasan *et al*., 2015**). **Dong *et al*. (2013)** studied the drag difference between a normal surface and a hydrodynamic surface, and they found that the superhydrophobic surface with static CA of 159.7° could reduce the drag force up to 49.1%, compared with the normal surface. Thus, applying antifouling coatings with hydrophobic surfaces would have combined benefits of enhanced antifouling and hydrodynamic drag reduction.

Another useful application for hydrophobic coatings is for deicing. Ice formed on a surface is due to surface adhesion that retains the water droplets. Hydrophobic surfaces can repel water and have low adhesion, and this can delay the formation of ice and ease the mechanical ice removal (**Nazhipkyzy *et al*., 2016**). In addition, for self-induced deicing on a surface, ice removal usually starts when solid-ice melts into water at the interface; while water is super slick on the hydrophobic surface, thus enabling excellent deicing performance (**Nine *et al*., 2017**).

Self-Healing Coatings and Their Applications

Polymer coatings are attractive due to their cost effective and excellent performance in different applications. However, when used in actual environments, such as for solar panel protection, the polymer coatings could be eroded or scratched by the high speed abrasive sand particles in the wind (**Humood *et al*., 2017**). In addition, the coatings may suffer from decomposition under sunlight (**Mozumder *et al*., 2019**). When coatings on solar panels suffer from such damages, transmittance and wettability will decline. Therefore, expensive and inconvenient interval renovations of the coatings is necessary (**Mozumder *et al*., 2019**). Inspired by natural plants, such as the lotus leaf that can repair its surface superhydrophobicity, even after damage by regrow of epicuticular wax tubules on the surface (**Neinhuis *et al*., 2001**), researchers have shown interest on coatings with self-healing capability, which would be cost-effective and efficient in actual applications (**Mozumder *et al*., 2019**). Specifically, anticorrosion has been one of most attractive applications for self-healing coatings (Cho *et al*., 2009; Samadzadeh *et al*., 2010; Yabuki and Okumura, 2012; Schreiner *et al*., 2017; Guo *et al*., 2018; Njoku *et al*., 2018).

Maintaining the functions of the coating is the main goal of self-healing, and there are mainly two different methods, namely physical and chemical methods, to achieve this goal. Physical self-healing does not involve any chemical reactions. For example, **Wong *et al*. (2011)** designed an omniphobic liquid film by using the nano/ microstructured substrates to lock in place the infused lubricating fluid: Because the liquid surface is intrinsically smooth and defect-free, the surrounding liquid can immediately wick into the scratched area and the surface is self-healed. In another example, Golovin, *et al.* fabricated a superhydrophobic coating that can maintain its hydrophobicity by expositing new micro structures after abrasion. In addition, the coating can regain its surface texture by immersing in heat even after 150 MPa pressure compression (**Golovin *et al*., 2017**). In the third example, Yabuki, *et al.* mixed a superabsorbent polymer (SAP) additive in the vinyl-ester polymer to coat on a metal substrate for corrosion protection. After scratch damage, the SAP in the composite coating could absorb water and the swelled SAP can prevent the diffusion of dissolved oxygen to reach the metal substrate and thus inhibits corrosion (Yabuki and Okumura, 2012; Yabuki *et al*., 2018).

Compared to physical self-healing, chemical self-healing is more active. Cho, *et al.* used a self-healing chemistry based on di-*n*-butyltin dilaurate catalyzed polycondensation of polydimethylsiloxane (PDMS) and polydiethoxysiloxane (PDES). As shown in **Fig. 12(a)**, the dimethyldineodecanoatetin (DMDNT) catalyst is microencapsulated and the PDMS-based healing agent (a mixture of 96 vol% HOPDMS and 4 vol% PDES) is distributed evenly as droplets on the coating outside of the microencapsulates. When the coating is damaged by scratch, as in **Fig. 12(b)**, the microencapsulates will break, the catalyst can flow to the scratch and contact with the healing agent. Once the catalyst mixes with the healing agent, as in **Fig. 12(c)**, they will react with each other and heal the scratch and protect the substrate from the environment (**Fig. 12(d)**). In the same study, Cho, *et al.* produced another self-healing coating by encapsulation of both the catalyst and the healing agent, which provided better corrosion protection, compared with the one shown in **Fig. 12(a)**.

There are different chemistries that can be used for self-healing coatings. Lu *et al.* showed that fabrication of composite material coatings with a healing agent could be a promising strategy which was effective, low-cost and easily scalable (Zhai *et al*., 2018; Zhou *et al*., 2018). According to **Hillewaere and Du Prez (2015)**, to achieve better healing efficiency, the self-healing chemistry needs to be accommodated with the coating matrix: for siloxane and azide-alkyne chemistry, they work well only in PDMS and polyisobutylene (PIB) matrix. To get a better mixture and cover over the damaged area, reducing the viscosity of the healing chemistry by adding a solvent improves the recovery. There are many different ways to produce the microcapsules for healing chemistry (Park and Braun, 2010; Najjar *et al*., 2018; Njoku *et al*., 2018; Zhang *et al*., 2018). For example, **Zhang *et al*. (2018)** produced Poly(urea-formaldehyde)-epoxy ester microcapsules through a two-step process in an oil-in-water emulsion: a shell pre-polymer solution was formed in the first step; in the second step, the epoxy was added in the solution and then agitated to an emulsion status, then by changing the temperature and PH, the pre-polymer will consolidate on the surface of the ester droplets and form the ester microcapsules.

In another work, **Park and Braun (2010)** applied a coaxial electrospinning method to form the capsule for self-healing chemistry and this is a purely physical approach to form the core/sheath structure. As shown in **Fig. 13(a)** depicting the schematic for the coaxial electrospinning

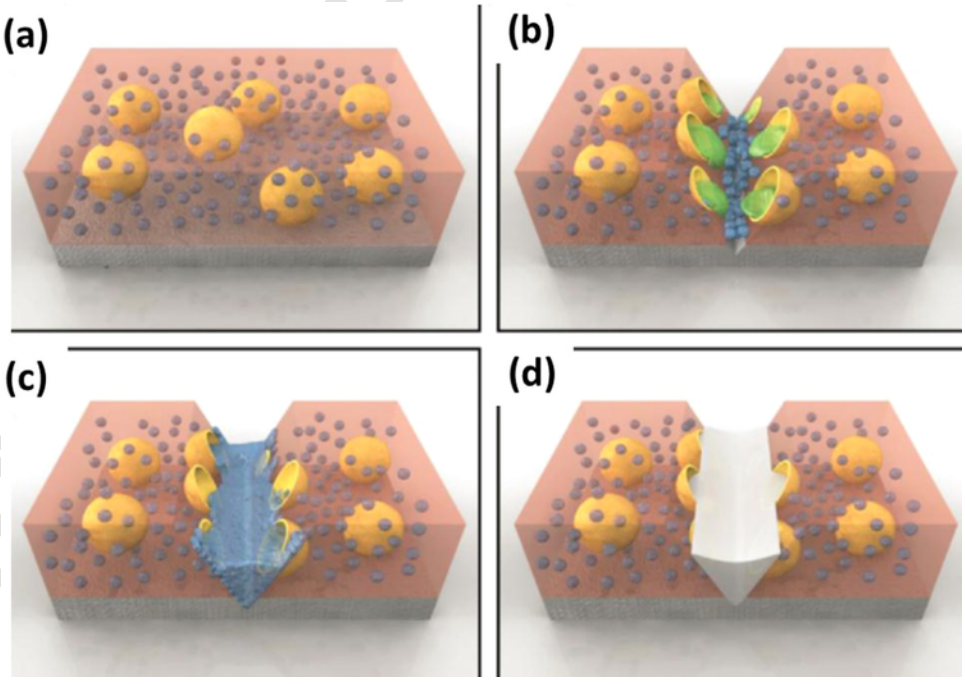

Fig. 12 Schematic of self-healing process, (a) Self-healing coating containing microencapsulated catalyst (yellow) and phase-separated healing agent droplets (blue) in the coating, (b) Damage to the coating layer releases catalyst (green) and healing agent (blue). (c) Mixing of healing agent and catalyst in the damaged region, (d) Damage healed by cross-linked PDMS, protecting the substrate from the environment. Modified from Cho, S.H., White, S.R., Braun, P.V., 2009. Self-healing polymer coatings. Advanced Materials 21 (6), 645–649.

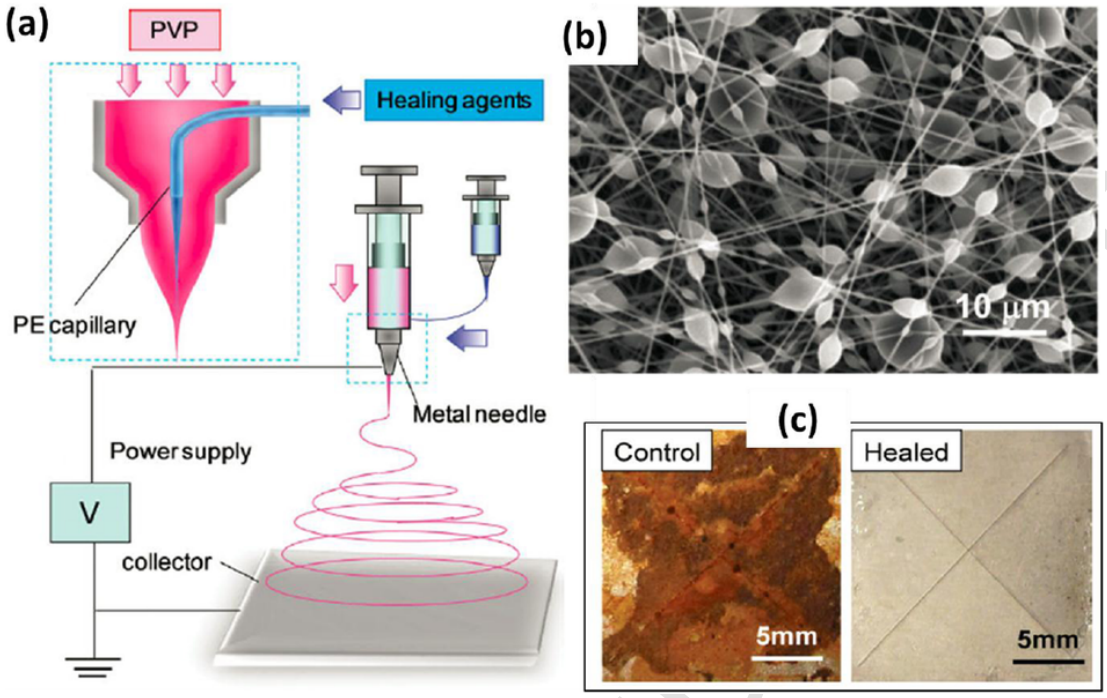

Fig. 13 Coaxial electrospinning of self-healing coating system, (a) the coaxial electrospinneret and fiber spinning process, (b)SEM image of as-spun core–shell bead-on-string morphology, (c) Photographs of control and self-healing coating samples that were stored under ambient conditions for 2 months after 5 days salt water immersion. Modified from Park, J.H., Braun, P.V., 2010. Coaxial electrospinning of self-healing coatings. Advanced Materials 22 (4), 496–499.

system, two viscous liquids, namely the shell polymer and healing agents (two-part healing agent system), are feed through the inner and outer capillaries, respectively. By controlling the feeding liquids and other operational conditions, the healing agents can be encapsulated in the beads along with polymer nanofibers, as shown in **Fig. 13(b)** of the randomly orientated core–shell bead-on-string morphology, with two different healing agents in the bead and string shell. After the deposition of the electrospun fiber mat, a UV curing resin was sup-cast on the fiber mat and then cured as self-healing coating. **Fig. 13(c)** shows the control and self-healing coating samples after initial scratch and aging in corrosion environments, which clearly prove the effectiveness of the healing performance (**Park and Braun, 2010**).

The above mentioned chemical self-healing methods are based on repairing the coating by chemical reaction of the healing agents and forming a new layer on the damaged area. Rather than using the healing agents' reaction, another chemical self-healing method is the continually releasing of functional chemicals, such as anticorrosion agents, in the damaged area where no protection can be supplied by the physical coating coverage. To extend the service life after damage, the functional chemicals need to be released gradually from the carriers, such as haloysite nanotubes (HNT) (**Zahidah *et al*., 2017**), cellulose nanofibers (**Yabuki *et al*., 2016**) and polymer core–shell nanocontainers (**Li *et al*., 2014**). HNT material is abundantly available in nature and it can significantly extend the release time of an anticorrosion agent in water (**Zahidah *et al*., 2017**). As shown in **Fig. 14(a) and (b)** of the HNT morphology, the anticorrosion agent is able to stay in the hollow nanotubes. **Fig. 14(c)** shows the loading and coating process for HNT.

Under vacuum, the mixture of HNT and the anticorrosion agent was stirred and thus the agent was loaded in the nanotubes. In the next two steps, the loaded HNT was coated with double polyelectrolyte, namely Poly(allylaminehydrochloride) (PAH) and poly(styrene sulfonate) (PSS), respectively. When used in coating applications, the PAH and PSS films can form porous structures and then gradually release the anticorrosion agent from HNT to protect the metal substrate (**Dong *et al*., 2018**). Rather than load the anticorrosion agent in side hollow nanotubes, Yabuki *et al.* coated corrosion inhibitors on the surface of the cellulose nanofibers, then the coated nanofibers were mixed with a base polymer and then deposited on the metal surface (Yabuki *et al*., 2014; Yabuki *et al*., 2016). When scratch occurs, the corrosion inhibitor is gradually released along the nanofibers pathway, thus protecting the substrate (**Yabuki *et al*., 2014**). In addition, by changing the PH value of the coating, the release speed of corrosion inhibitor can be controlled (**Yabuki *et al*., 2016**).

Conclusions

In this article, different advanced polymeric coatings and their applications were reviewed, and the following conclusions could be drawn:

(1) High bearing blended polymer coatings based on PEEK, PTFE, and ATSP materials show promising tribological behavior under aggressive contact conditions. Even in the absent of liquid lubrication, in applications such as air-conditioning and refrigeration

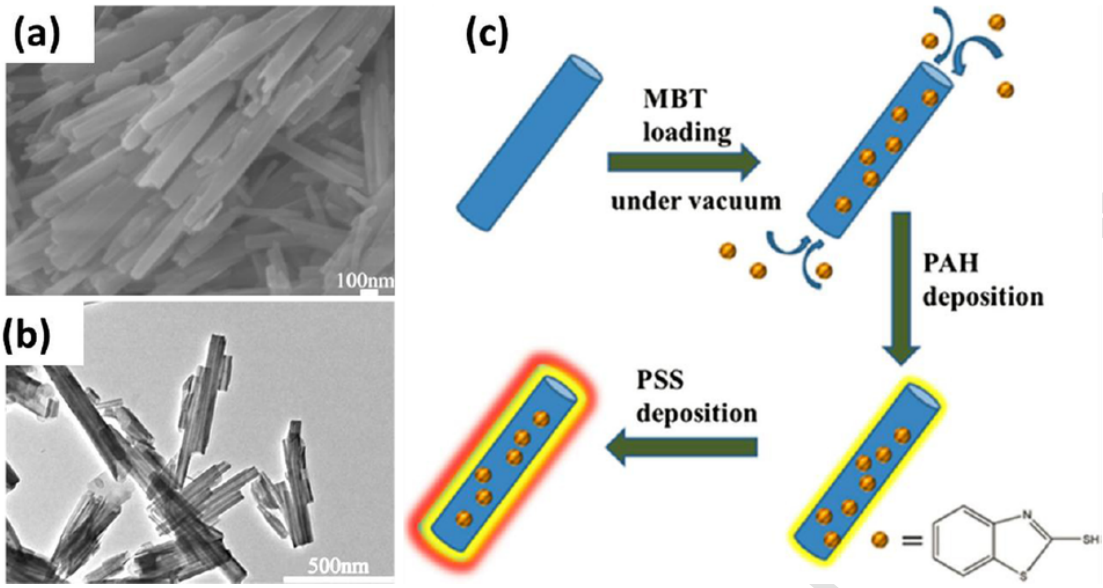

Fig. 14 HNT Nanocontainer for anticorrosion agent, (a) SEM image of HNT, (b) TEM image of HNT, (c) Process of loading and coating of HNT. Modified from Dong, C., Zhang, M., Xiang, T., *et al*., 2018. Novel self-healing anticorrosion coating based on L-valine and MBT-loaded halloysite nanotubes. Journal of Materials Science 53 (10), 7793–7808.

compressors, electrical submersible pumps, and under cryogenic conditions, they proved their suitability to withstand demanding contact and sliding conditions at the interface, while maintaining friction and wear at acceptable levels;

(2) One of the key aspects in the performance of high bearing blended polymer coatings is their ability to provide self-lubricity at the contact interface, by trapping wear debris or third bodies at the contact interface. Keeping these third bodies is what avoids/retards scuffing adhesive phenomena under stringent sliding conditions;

(3) Electrostatic deposition is one of the most cost/effective methods to coat metallic engineering substrates with polymer coatings. Compared to techniques such as thermal spray, electrostatically deposited coatings proved to perform well under aggressive conditions; and

(4) Both superhydrophobic and self-healing coatings using special chemistry and structure are used to fulfil their desired properties. Both coatings are using green technologies that can reduce labor cost and reduce environmental impact to maintain the coatings' functionality. Superhydrophobic coatings are more attractive for self-cleaning applications and self-healing coatings are more attractive for anticorrosion applications.

References

Akram, M.W., Polychronopoulou, K., Polycarpou, A.A., 2014. Tribological performance comparing different refrigerant– lubricant systems: The case of environmentally friendly HFO-1234yf refrigerant. Tribology International 78, 176–186.

Akram, M.W., Polychronopoulou, K., Seeton, C., Polycarpou, A.A., 2013. Tribological performance of environmentally friendly refrigerant HFO-1234 yf under starved lubricated conditions. Wear 304 (1–2), 191–201.

Anand, A., Haq, M.I.U., Vohra, K., Raina, A., Wani, M., 2017. Role of green tribology in sustainability of mechanical systems: A State of the art survey. Materials Today: Proceedings 4 (2), 3659–3665.

Arianpour, F., Farzaneh, M., Jafari, R., 2016. Hydrophobic and ice-phobic properties of self-assembled monolayers (SAMs) coatings on AA6061. Progress in Organic Coatings 93, 41–45.

Assadi, H., Schmidt, T., Richter, H., et al., 2011. On parameter selection in cold spraying. Journal of thermal spray technology 20 (6), 1161–1176.

Bach, F.-W., Möhwald, K., Laarmann, A., Wenz, T., 2006. Modern Surface Technology. John Wiley & Sons.

Bahadur, S., 2000. The development of transfer layers and their role in polymer tribology. Wear 245 (1–2), 92–99.

Barthlott, W., Neinhuis, C., 1997. Purity of the sacred lotus, or escape from contamination in biological surfaces. Planta 202 (1), 1–8.

Berretta, S., Ghita, O., Evans, K.E., 2014. Morphology of polymeric powders in Laser Sintering (LS): From Polyamide to new PEEK powders. European Polymer Journal 59, 218–229.

Cannaday, M., Polycarpou, A., 2006. Advantages of CO_2 compared to R410a refrigerant of tribologically tested Aluminum 390-T6 surfaces. Tribology Letters 21 (3), 185–192.

Champagne, V., Helfritch, D., 2014. Mainstreaming cold spray–push for applications. Surface Engineering 30 (6), 396–403.

Cho, S.H., White, S.R., Braun, P.V., 2009. Self-healing polymer coatings. Advanced Materials 21 (6), 645–649.

Danglad-Flores, J., Eickelmann, S., Riegler, H., 2018. Deposition of polymer films by spin casting: A quantitative analysis. Chemical Engineering Science 179, 257–264.

Dascalescu, D., Polychronopoulou, K., Polycarpou, A., 2009. The significance of tribochemistry on the performance of PTFE-based coatings in CO_2 refrigerant environment. Surface and Coatings Technology 204 (3), 319–329.

Davis, J., 2001. Introduction to thermal spray processing. In: Handbook of Thermal Spray Technology. ASM Innternational and Thermal Spray Society.
Demas, N.G., Polycarpou, A.A., 2008. Tribological performance of PTFE-based coatings for air-conditioning compressors. Surface and Coatings Technology 203 (3–4), 307–316.
Demas, N.G., Polycarpou, A.A., Conry, T.F., 2005. Tribological studies on scuffing due to the influence of carbon dioxide used as a refrigerant in compressors. Tribology Transactions 48 (3), 336–342.
Dong, C., Zhang, M., Xiang, T., et al., 2018. Novel self-healing anticorrosion coating based on L-valine and MBT-loaded halloysite nanotubes. Journal of Materials Science 53 (10), 7793–7808.
Dong, H., Cheng, M., Zhang, Y., Wei, H., Shi, F., 2013. Extraordinary drag-reducing effect of a superhydrophobic coating on a macroscopic model ship at high speed. Journal of Materials Chemistry A 1 (19), 5886–5891.
Donnet, C., Erdemir, A., 2004. Historical developments and new trends in tribological and solid lubricant coatings. Surface and Coatings Technology 180, 76–84.
Fender, T., 1996. Thermal spray high performance polymer coatings. Materials Technology 11 (1), 16–20.
Fenero, M., Palenzuela, J., Azpitarte, I., et al., 2017. Laponite-based surfaces with holistic self-cleaning functionality by combining antistatics and omniphobicity. ACS Applied Materials & Interfaces 9 (44), 39078–39085.
Frich, D., Economy, J., 1997. Thermally stable liquid crystalline thermosets based on aromatic copolyesters: Preparation and properties. Journal of Polymer Science Part A: Polymer Chemistry 35 (6), 1061–1067.
Frich, D., Goranov, K., Schneggenburger, L., Economy, J., 1996. Novel high-temperature aromatic copolyester thermosets: synthesis, characterization, and physical properties. Macromolecules 29 (24), 7734–7739.
Friedrich, K., 2018. Polymer composites for tribological applications. Advanced Industrial and Engineering Polymer Research 1, 3–39.
Friedrich, K., Theiler, G., Klein, P., 2009. Polymer composites for tribological applications in a range between liquid helium and room temperature. Polymer Tribology 375–415.
Gao, X., Hu, M., Fu, Y., et al., 2018. Response of MoS_2-Sb_2O_3 film to low-earth-orbit space environment. Materials Letters 227, 161–164.
Golovin, K., Boban, M., Mabry, J.M., Tuteja, A., 2017. Designing self-healing superhydrophobic surfaces with exceptional mechanical durability. ACS Applied Materials & Interfaces 9 (12), 11212–11223.
Grill, A., 1993. Review of the tribology of diamond-like carbon. Wear 168 (1–2), 143–153.
Guo, M., Li, W., Han, N., et al., 2018. Novel dual-component microencapsulated hydrophobic amine and microencapsulated isocyanate used for self-healing anti-corrosion coating. Polymers 10 (3), 319.
Hillewaere, X.K., Du Prez, F.E., 2015. Fifteen chemistries for autonomous external self-healing polymers and composites. Progress in Polymer Science 49, 121–153.
Humood, M., Beheshti, A., Polycarpou, A.A., 2017. Surface reliability of annealed and tempered solar protective glasses: Indentation and scratch behavior. Solar Energy 142, 13–25.
Koch, K., Bhushan, B., Jung, Y.C., Barthlott, W., 2009. Fabrication of artificial Lotus leaves and significance of hierarchical structure for superhydrophobicity and low adhesion. Soft Matter 5 (7), 1386–1393.
Kondyurina, I., Kondyurin, A., Lauke, B., Vogel, R., Reuter, U., 2006. Polymerisation of composite materials in space environment for development of a Moon base. Advances in Space Research 37 (1), 109–115.
Lan, P., Polycarpou, A.A., 2018. High temperature and high pressure tribological experiments of advanced polymeric coatings in the presence of drilling mud for oil & gas applications. Tribology International 120, 218–225.
Lan, P., Meyer, J.L., Economy, J., Polycarpou, A.A., 2016. Unlubricated tribological performance of aromatic thermosetting polyester (ATSP) coatings under different temperature conditions. Tribology Letters 61 (1), 10.
Lan, P., Polychronopoulou, K., Zhang, Y., Polycarpou, A.A., 2017. Three-body abrasive wear by (silica) sand of advanced polymeric coatings for tilting pad bearings. Wear 382, 40–50.
Lan, P., Gheisari, R., Meyer, J.L., Polycarpou, A.A., 2018. Tribological performance of aromatic thermosetting polyester (ATSP) coatings under cryogenic conditions. Wear 398, 47–55.
Li, G.L., Schenderlein, M., Men, Y., Möhwald, H., Shchukin, D.G., 2014. Monodisperse polymeric core–shell nanocontainers for organic self-healing anticorrosion coatings. Advanced Materials Interfaces 1 (1), 1300019.
Michael, P., Rabinowicz, E., Iwasa, Y., 1991. Friction and wear of polymeric materials at 293, 77 and 4.2 K. Cryogenics 31 (8), 695–704.
Mozumder, M.S., Mourad, A.-H.I., Pervez, H., Surkatti, R., 2019. Recent developments in multifunctional coatings for solar panel applications: A review. Solar Energy Materials and Solar Cells 189, 75–102.
Myshkin, N., Petrokovets, M., Kovalev, A., 2005. Tribology of polymers: adhesion, friction, wear, and mass-transfer. Tribology International 38 (11–12), 910–921.
Najjar, R., Akbari, M., Mirmohseni, A., Hosseini, M., 2018. Preparation and corrosion performance of healable waterborne polyurethane coatings containing isophoronediisocyanate loaded silica capsules. Journal of the Taiwan Institute of Chemical Engineers
Nazhipkyzy, M., Mansurov, Z., Amirfazli, A., et al., 2016. Influence of superhydrophobic properties on deicing. Journal of Engineering Physics and Thermophysics 89 (6), 1476–1481.
Neinhuis, C., Koch, K., Barthlott, W., 2001. Movement and regeneration of epicuticular waxes through plant cuticles. Planta 213 (3), 427–434.
Nine, M.J., Cole, M.A., Johnson, L., Tran, D.N., Losic, D., 2015. Robust superhydrophobic graphene-based composite coatings with self-cleaning and corrosion barrier properties. ACS Applied Materials & Interfaces 7 (51), 28482–28493.
Nine, M.J., Tung, T.T., Alotaibi, F., Tran, D.N., Losic, D., 2017. Facile adhesion-tuning of superhydrophobic surfaces between “lotus” and “petal” effect and their influence on icing and deicing properties. ACS Applied Materials & Interfaces 9 (9), 8393–8402.
Njoku, C.N., Arukalam, I.O., Bai, W., Li, Y., 2018. Optimizing maleic anhydride microcapsules size for use in self-healing epoxy-based coatings for corrosion protection of aluminum alloy. Materials and Corrosion 69 (9), 1257–1267.
Nosonovsky, M., Ramachandran, R., 2015. Geometric interpretation of surface tension equilibrium in superhydrophobic systems. Entropy 17 (7), 4684–4700.
Nunez, E.E., Polycarpou, A.A., 2015. The effect of surface roughness on the transfer of polymer films under unlubricated testing conditions. Wear 326, 74–83.
Nunez, E.E., Gheisari, R., Polycarpou, A.A., 2019. Tribology review of blended bulk polymers and their coatings for high-load bearing applications. Tribology International 129, 92–111.
Nunez, E.E., Demas, N.G., Polychronopoulou, K., Polycarpou, A.A., 2008. Tribological study comparing PAG and POE lubricants used in air-conditioning compressors under the presence of CO_2. Tribology Transactions 51 (6), 790–797.
Nunez, E.E., Demas, N.G., Polychronopoulou, K., Polycarpou, A.A., 2010. Comparative scuffing performance and chemical analysis of metallic surfaces for air-conditioning compressors in the presence of environmentally friendly CO_2 refrigerant. Wear 268 (5–6), 668–676.
Nunez, E.E., Yeo, S.M., Polychronopoulou, K., Polycarpou, A.A., 2011. Tribological study of high bearing blended polymer-based coatings for air-conditioning and refrigeration compressors. Surface and Coatings Technology 205 (8–9), 2994–3005.

Ovaert, T., Cheng, H., 1991. Counterface topographical effects on the wear of polyetheretherketone and a polyetheretherketone-carbon fiber composite. Wear 150 (1–2), 275–287.
Park, J.H., Braun, P.V., 2010. Coaxial electrospinning of self-healing coatings. Advanced Materials 22 (4), 496–499.
Petrovicova, E., Schadler, L., 2002. Thermal spraying of polymers. International Materials Reviews 47 (4), 169–190.
Pippin, G., 2003. Space environments and induced damage mechanisms in materials. Progress in Organic Coatings 47 (3–4), 424–431.
Raletz, F., Vardelle, M., Ezoʻo, G., 2006. Critical particle velocity under cold spray conditions. Surface and Coatings Technology 201 (5), 1942–1947.
Samadzadeh, M., Boura, S.H., Peikari, M., Kasiriha, S., Ashrafi, A., 2010. A review on self-healing coatings based on micro/nanocapsules. Progress in Organic Coatings 68 (3), 159–164.
Sasaki, S., 2010. Environmentally friendly tribology (eco-tribology). Journal of Mechanical Science and Technology 24 (1), 67–71.
Schreiner, C., Scharf, S., Stenzel, V., Rössler, A., 2017. Self-healing through microencapsulated agents for protective coatings. Journal of Coatings Technology and Research 14 (4), 809–816.
Selim, M.S., Shenashen, M.A., Elmarakbi, A., et al., 2017. Synthesis of ultrahydrophobic and thermally stable inorganic–organic nanocomposites for self-cleaning foul release coatings. Chemical Engineering Journal 320, 653–666.
Selim, M.S., Yang, H., Wang, F.Q., et al., 2018. Silicone/Ag@ SiO_2 core–shell nanocomposite as a self-cleaning antifouling coating material. RSC Advances 8 (18), 9910–9921.
Selim, M.S., El-Safty, S.A., Fatthallah, N.A., Shenashen, M.A., 2018. Silicone/graphene oxide sheet-alumina nanorod ternary composite for superhydrophobic antifouling coating. Progress in Organic Coatings 121, 160–172.
Shaffer, S., Rogers, M., 2007. Tribological performance of various coatings in unlubricated sliding for use in small arms action components – A case study. Wear 263 (7–12), 1281–1290.
Srinivasan, S., Kleingartner, J.A., Gilbert, J.B., et al., 2015. Sustainable drag reduction in turbulent Taylor-Couette flows by depositing sprayable superhydrophobic surfaces. Physical Review Letters 114 (1), 014501.
Tuteja, A., Choi, W., Mabry, J.M., McKinley, G.H., Cohen, R.E., 2008. Robust omniphobic surfaces. Proceedings of the National Academy of Sciences 105 (47), 18200–18205.
Vyawahare, S.M., 2006. Protective thermal spray coatings for polymer matrix composites, Thesis (M.S.), Wichita State University.
Wang, Q., 1997. Seizure failure of journal-bearing conformal contacts. Wear 210 (1–2), 8–16.
Wang, Q., Zheng, F., Wang, T., 2016. Tribological properties of polymers PI, PTFE and PEEK at cryogenic temperature in vacuum. Cryogenics 75, 19–25.
Wong, T.-S., Kang, S.H., Tang, S.K., et al., 2011. Bioinspired self-repairing slippery surfaces with pressure-stable omniphobicity. Nature 477 (7365), 443.
Xiao, L., Deng, M., Zeng, W., et al., 2017. Novel robust superhydrophobic coating with self-cleaning properties in air and oil based on rare earth metal oxide. Industrial & Engineering Chemistry Research 56 (43), 12354–12361.
Yabuki, A., Okumura, K., 2012. Self-healing coatings using superabsorbent polymers for corrosion inhibition in carbon steel. Corrosion Science 59, 258–262.
Yabuki, A., Kawashima, A., Fathona, I.W., 2014. Self-healing polymer coatings with cellulose nanofibers served as pathways for the release of a corrosion inhibitor. Corrosion Science 85, 141–146.
Yabuki, A., Shiraiwa, T., Fathona, I.W., 2016. pH-controlled self-healing polymer coatings with cellulose nanofibers providing an effective release of corrosion inhibitor. Corrosion Science 103, 117–123.
Yabuki, A., Tanabe, S., Fathona, I.W., 2018. Self-healing polymer coating with the microfibers of superabsorbent polymers provides corrosion inhibition in carbon steel. Surface and Coatings Technology 341, 71–77.
Yeo, S.M., Polycarpou, A.A., 2012. Tribological performance of PTFE-and PEEK-based coatings under oil-less compressor conditions. Wear 296 (1–2), 638–647.
Yeo, S.M., Polycarpou, A.A., 2013. Micromechanical properties of polymeric coatings. Tribology International 60, 198–208.
Yeo, S.M., Polycarpou, A.A., 2014. Fretting experiments of advanced polymeric coatings and the effect of transfer films on their tribological behavior. Tribology International 79, 16–25.
Yeo, S.M., Escobar Nunez, E., Polycarpou, A.A., 2010. Tribological performances of polymer-based coating materials designed for compressor applications. In: Advances in Science and Technology. Trans Tech Publication, pp. 33–42.
Zahidah, K.A., Kakooei, S., Ismail, M.C., Raja, P.B., 2017. Halloysite nanotubes as nanocontainer for smart coating application: A review. Progress in Organic Coatings 111, 175–185.
Zhai, W., Lu, W., Zhang, P., et al., 2018. Wear-triggered self-healing behavior on the surface of nanocrystalline nickel aluminum bronze/Ti_3SiC_2 composites. Applied Surface Science 436, 1038–1049.
Zhang, C., Wang, H., Zhou, Q., 2018. Preparation and characterization of microcapsules based self-healing coatings containing epoxy ester as healing agent. Progress in Organic Coatings 125, 403–410.
Zhang, G., Liao, H., Yu, H., et al., 2006. Deposition of PEEK coatings using a combined flame spraying–laser remelting process. Surface and Coatings Technology 201 (1–2), , 243–249.
Zhang, G., Liao, H., Yu, H., et al., 2006. Correlation of crystallization behavior and mechanical properties of thermal sprayed PEEK coating. Surface and Coatings Technology 200 (24), 6690–6695.
Zhang, J., 2008. Design of polymer composites with improved adhesion and wear properties, Thesis (Dr.), University of Illinois at Urbana-Champaign.
Zhou, M., Lu, W., Liu, X., et al., 2018. Fretting wear properties of plasma-sprayed Ti3SiC2 coatings with oxidative crack-healing feature. Tribology International 118, 196–207.